

# Use of proximity transducers for local radial strain measurements in a hollow cylinder apparatus

O'Kelly, B.C.

*Department of Civil, Structural and Environmental Engineering, Trinity College Dublin, Dublin 2, Ireland*

Naughton, P.J.

*School of Engineering, Institute of Technology, Sligo; Sligo, Ireland*

**Keywords:** calibration, hollow cylinder apparatus, instrumentation, proximity transducer

**ABSTRACT:** This paper describes the use of proximity transducers to accurately measure the radial and circumferential normal strains of the test specimen (covering the pseudo elastic range to shear failure) in a hollow cylinder apparatus. The non-contact proximity transducers, which were located in the outer cell chamber and the inner bore cavity of the specimen, measure the radial displacements of the inner and outer specimen wall surfaces over a central, uniformly stressed zone. The waterproofing and set up of the transducers, including the precision gearing that is used to relocate the instruments from outside the pressure cell during the course of a test, are described. The transducers, which have a measurement range of 6.0 mm and a resolution of  $1.1 \times 10^{-6}$  mm, were calibrated in water to an accuracy of  $1.0 \times 10^{-5}$  mm (radial and circumferential normal strains of  $7 \times 10^{-5}$  %) using an optical table and a laser distance measurement system. The calibration data was non linear and strongly influenced by the target curvature (convex and concave for the outer and inner wall surfaces, respectively). Generalized stress path tests were carried out on fully saturated sand specimens and the deformation response was measured using the local (proximity transducers) and external instrumentation. The external measurements included significant errors, particularly in the case of the outer wall displacement, due to: (a) apparatus compliance; (b) specimen end restraint and bedding effects; (c) inaccuracies in measuring the volume change of the specimen and its inner bore cavity and (d) the fact that the wall displacements were calculated as mean values over the full specimen volume.

## 1 INTRODUCTION

It is now widely recognized that local instrumentation should be used to measure the load–deformation response of a geomaterial specimen in the triaxial apparatus to obtain an accurate assessment of the small strain stiffness response. Measurement errors due to apparatus compliance and specimen end-restraint and bedding effects are excluded when the specimen deformations are measured over a central gage length (Jardine et al. 1984; Baldi et al. 1988).

Many innovative techniques have been developed to locally measure axial specimen deformations including, for example, LVDTs (Cuccovillo and Coop, 1997); electrolevel inclinometers (Jardine et al. 1984; Symes and Burland, 1984) and Hall-effect transducers (Clayton and Khatrush, 1986). However, the attachment of the instruments to the specimen wall surface may influence the deformation response, particularly during dynamic load testing.

Image analysis (Rechenmacher and Finno, 2004) and non-contacting electromagnetic techniques, for example, proximity transducers (Brown et al. 1980; Symes and Burland, 1984; Hird and Yung, 1989; Lo Presti et al. 1993; Menkiti, 1995; among others) offer some advantage in this respect.

The technology of proximity transducers is well developed and a wide range of equipment is commercially available. Proximity transducers have been used for many applications in geotechnical laboratory testing. The transducers use the principle of impedance variation (eddy current loss) to measure the gap between the transducer face and an aluminum foil target that has been attached to the rubber membrane that encloses the specimen wall surface. The transducer coil constitutes one leg of a balanced Wheatstone bridge network. The bridge network senses changes in the impedance of the transducer coil as the foil target moves within the electromagnetic field and the data is converted to an analogue voltage by a signal-conditioning unit.

Hird and Yung (1989) reported a measurement resolution of  $1.0 \times 10^{-3}$  mm for a proximity transducer with a 5.0 mm range. Resolutions of  $2.5 \times 10^{-5}$  mm (Scholey et al. 1995) and  $3.0 \times 10^{-4}$  mm (Lo Presti et al. 1993) have been reported for proximity transducers with a measurement range of 2.5 mm. A measurement accuracy of  $1.0 \times 10^{-3}$  mm has also been reported by Lo Presti et al. (1993).

The aluminum foil target (less than 0.02 mm in thickness) is attached by smearing the outside of the rubber membrane with silicone grease, which prevents any reinforcement effect on the specimen. The displacement of the membrane, and hence the foil target, matches that of the specimen wall surface (Tatsuoka et al. 1983). An allowance is made in sizing the foil target to accommodate the anticipated relative movements between the transducer face and the specimen wall surface during the course of a test.

The particular focus of this paper is the setup, waterproofing, performance and calibration of the proximity transducers that measure the radial displacements of the hollow cylindrical specimen (35.5 mm inner radius; 50.0 mm outer radius and 200.0 mm in length) tested in the University College Dublin (UCD) hollow cylinder apparatus (HCA) developed by O'Kelly and Naughton (2003; 2005b), Fig. 1.

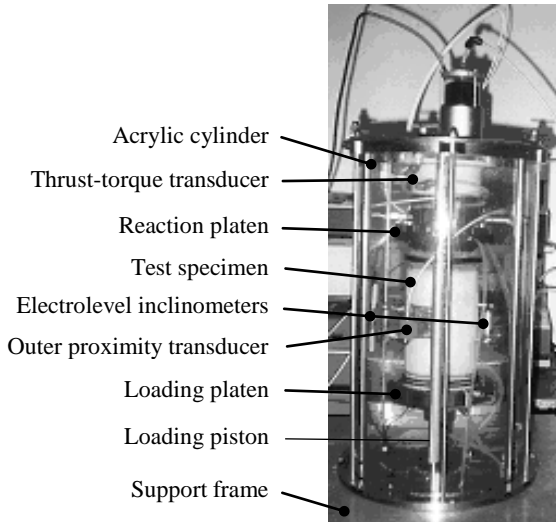


Figure 1. Cell of UCD hollow cylinder apparatus.

Independently-controlled confining pressures are applied to the outer cell chamber and the inner bore cavity of the specimen. A system of axial and torsional loads is applied via ribbed, sintered bronze discs in contact with the lower end of the specimen which is fully restrained at its upper end.

Specific objectives of this study include: (a) Development of data acquisition hardware and calibration procedures to achieve the necessary resolution and accuracy for strain measurements over the pseudo elastic range; (b) Study the effects of the curvature of the specimen wall surfaces and the operating

environment (in air or submerged under water) on the transducer calibration; (c) Assess the level of the error in the radial wall deformations recorded using instrumentation located outside the pressure cell.

## 2 MEASUREMENT OF DEFORMATION RESPONSE IN UCD HCA

The polar deformation response of the specimen is measured within the uniformly stressed zone near the specimen mid-height (Naughton and O'Kelly, 2007) to a resolution of better than  $5 \times 10^{-5}$  strain using proximity transducers and electrolevel inclinometers. Similar instrumentation was used by Hight et al. (1983) in the large Imperial College HCA, although in this case, the test specimen was 101.5 mm in inner radius, 127.0 mm in outer radius and 254 mm in length.

In the UCD HCA, three electrolevel inclinometers, which had been modified to suit the UCD HCA setup (O'Kelly and Naughton, 2008), are attached to the outer specimen membrane in order to measure the axial and torsional shear deformations over a central gage (initially 40 mm in length). Two proximity transducers measure the radial displacements of the outer and inner specimen wall surfaces.

Measurements of the overall deformation response are also recorded using instrumentation located outside the pressure cell (O'Kelly and Naughton, 2005). For example, the radial displacements of the inner and outer specimen wall surfaces can be calculated from the volume changes of the specimen and its inner bore cavity (independently measured by pressure-volume controllers manufactured by GDS Instruments Limited, UK) and the axial deformation measured over the full length of the specimen by displacement transducers.

The mean radial and circumferential normal strains ( $\varepsilon_r$  and  $\varepsilon_\theta$ ) developed across the specimen wall thickness are computed from the radial displacements of the outer and inner specimen wall surfaces ( $u_o$  and  $u_i$ , respectively) measured by the two proximity transducers (Eqs. 1, 2).

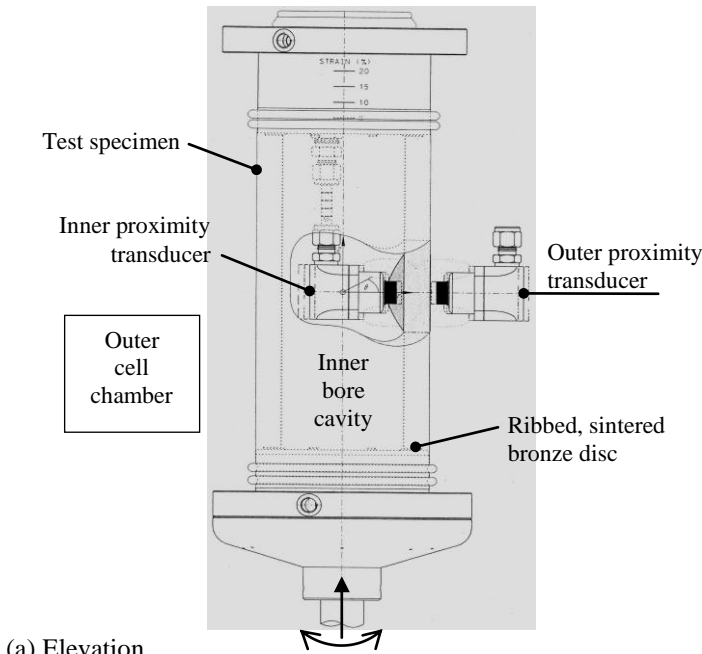
$$\overline{\varepsilon_r} = - \left( \frac{u_o - u_i}{r_o - r_i} \right) \quad (1)$$

$$\overline{\varepsilon_\theta} = - \left( \frac{u_o + u_i}{r_o + r_i} \right) \quad (2)$$

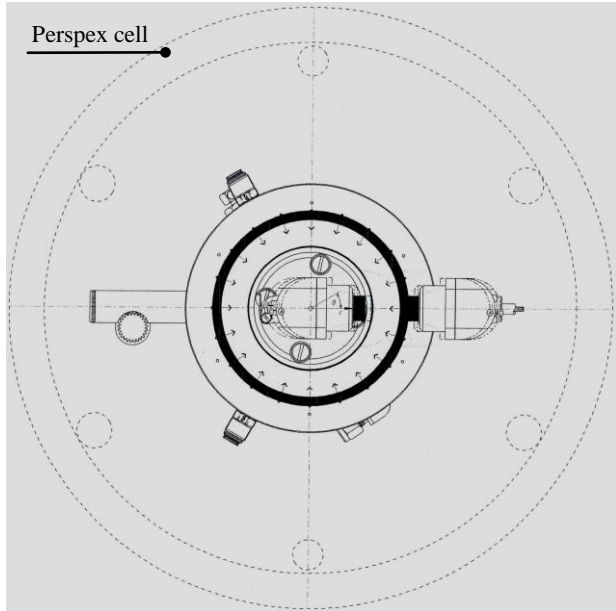
where  $r_o$  is the initial radius of the outer specimen wall surface (measured to 0.1 mm using  $\pi$  tape) and  $r_i$  is the initial radius of the inner specimen wall surface (calculated to 0.1 mm from the recorded water depth on filling the inner bore cavity with a known water volume during set up).

### 3 SET UP OF PROXIMITY TRANSDUCERS IN UCD HCA

The radial displacements of the inner and outer specimen wall surfaces are measured using two proximity transducers, one of which is located in the outer cell chamber while the second is located directly opposite inside the inner bore cavity, Fig. 2.



(a) Elevation.



(b) Plan.

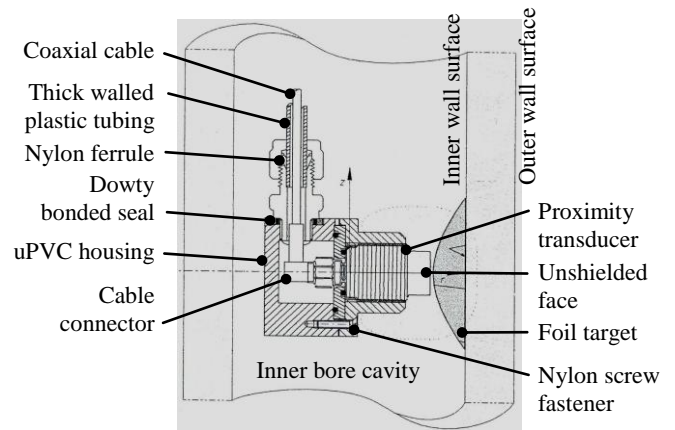
Figure 2. Setup of proximity transducers inside and outside the specimen.

The proximity transducers can be located at different elevations. The location of the transducers shown in Fig. 2a corresponds to the specimen mid-height, which is the usual setup during a test. The gap between the transducer face and the foil target (attached to the specimen membrane) can be ad-

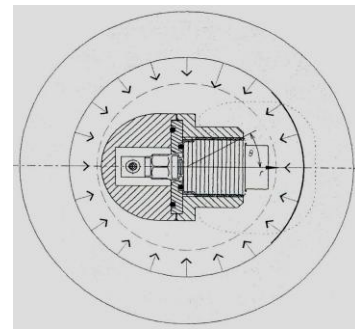
justed to accommodate the anticipated deformation response during the course of a test.

The proximity transducers (type 6U unshielded), which were manufactured by Kaman Instrumentation Corporation (USA), have a measurement range of 6.0 mm and a recommended transducer offset distance of between 0.6 and 1.2 mm.

The proximity transducers and right-angled cable connectors are electrically insulated inside compact uPVC housings that had been fastened together using nylon screw fasteners (Fig. 3).



(a) Sectional elevation.



(b) Plan.

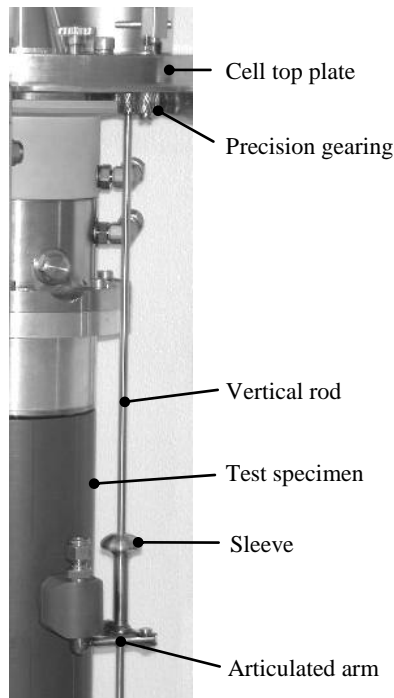
Figure 3. Section through inner proximity transducer housing.

A special micro-seal waterproofing treatment was applied to the face of the transducers. The coaxial cables (3.0 m in length) from the transducers form an integral part of the Wheatstone bridge circuit. The cables were sealed inside thick-walled plastic tubing that exits through the top plate of the pressure cell. Hand-tightened nylon ferrules, rubber O-rings and Dowty bonded seals hydraulically sealed the transducer housings.

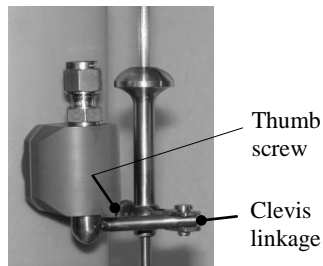
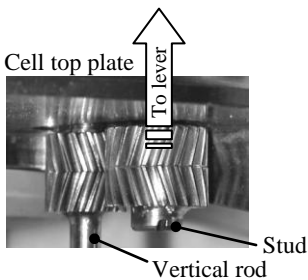
The transducer housing was specially profiled such that the assembly fitted neatly inside the inner bore cavity and allows radial contractions of the inner specimen wall of up to 9.4 mm (27% strain). Furthermore, the buoyant weight of the transducer mounted within its housing was negligible.

The location of the transducers can be adjusted from outside the pressure cell using precision gearing (operated from above the cell top plate) in order to suit the specimen deformation response during the course of a test. The outer proximity transducer

housing is supported by an articulated arm from a vertical rod (Fig. 4).



(a) Mechanism.



(b) Double-helical gears. (c) Housing support.  
Figure 4. Mechanism that locates outer proximity transducer.

Meshing double-helical gears hold the upper end of the vertical rod against the cell top plate (Fig. 4b) and facilitate fine adjustments of the housing location. The gear soldered to the top of the rod locates within a blind hole in the cell top plate. A stud attaches the second gear to a lever (located above the cell top plate) which operates the mechanism.

The mechanism that is operated through the reaction platen assembly to locate the proximity transducer inside the inner bore cavity is shown in Fig. 5.

During the assembly of the apparatus, the transducer is positioned at the mid-height of the specimen, perpendicular to its inner wall surface, before the inner cavity is sealed by securing the specimen top cap to the top reaction platen. Compression O-rings seal the two pressure chambers as well as vibration proofing the mechanism. The mechanism is operated from above the cell top plate by a lever and gearing (rack and pinion). A precision guide maintains the correct vertical alignment of the elbow that supports the transducer housing.

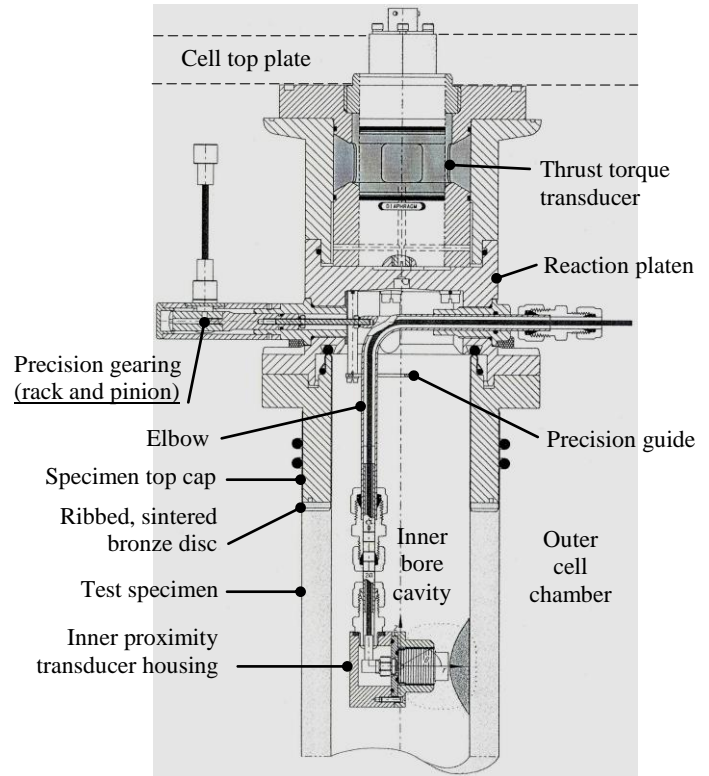


Figure 5. Mechanism that locates inner proximity transducer.

Neither the outer cell chamber nor the inner bore cavity experience a volume change as a result of the operator relocating the inner proximity transducer during the course of a test. Moreover, the net horizontal force that acts on the mechanism is zero (even when different outer and inner confining pressures are applied) since the rack and the elbow have equal cross-sectional area through the reaction platen. A locking device located above the cell top plate prevents accidental movement of the operating lever and hence the transducer during the course of a test.

#### 4 DATA ACQUISITION AND CONTROL

This section describes the data acquisition (DAQ) hardware that was used in conjunction with the proximity transducers in the UCD HCA. The closed-loop control of the apparatus using LabVIEW to target a prescribed stress path has been reported elsewhere by O'Kelly and Naughton (2005a).

The local instrumentation (electrolevel inclinometers and proximity transducers) was connected to a stand-alone 24-bit DAQ unit (National Instruments, NI4350) in order to achieve the necessary resolution for deformation measurements in the pseudo elastic range (strain levels less than 0.001% strain). The DAQ unit has eight differential inputs at reading rates of 2.8, 8.8 and 9.7 readings/s in multi acquisition mode.

The proximity transducers have a full-scale output of  $\pm 5.0$  volts so that the DAQ unit can resolve

the output to  $1.1 \times 10^{-6}$  mm (more than an order of magnitude improvement in the resolution values reported by Hird and Yung (1989), Scholey et al. (1995) and Lo Presti et al. (1993)).

The input and output signals from the local instrumentation (coaxial cables) were connected in differential mode to a general purpose terminal block (National Instruments, TBX68) which in turn was connected to the DAQ unit by a shielded cable, 1.0 m in length, also supplied by National Instruments. The DAQ unit was connected via a USB port to the control computer.

## 5 CALIBRATION

A special calibration procedure was developed for the proximity transducers to achieve the measurement accuracy necessary for measurements over the pseudo elastic range. The transducers were mounted in their uPVC housings and calibrated under water (in service condition) at atmospheric pressure.

The transducer response is influenced by its operating environment, with calibration under water producing a different response to calibration in air (Menkiti, 1995). Water is a polar fluid so that the transducer output is influenced by the dielectric constant of water. However, the operation of the transducers (variation in impedance) is not affected by the range of confining pressures that are applied to the cell chamber and the inner bore cavity.

The transducer housings were submerged under water and set up on an optical table that allowed set displacements to a resolution of 0.0025 mm in three orthogonal directions (Fig. 6).

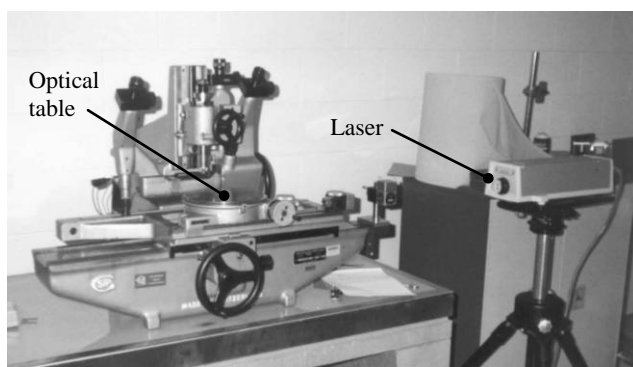
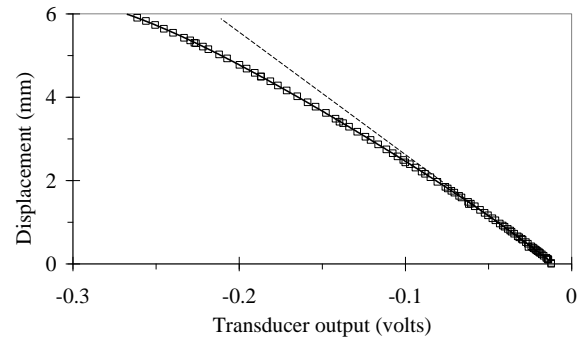


Figure 6. Optical table and laser distance measurement system.

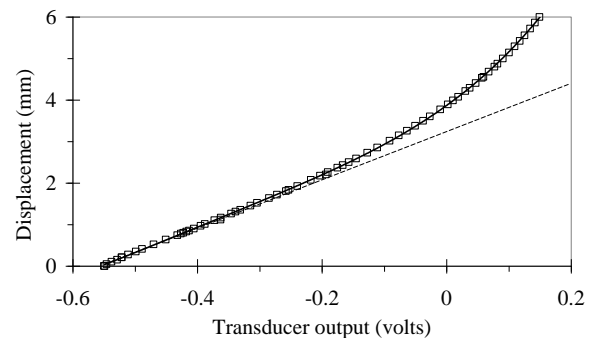
Two uPVC discs that had the same curvatures as the inner and outer wall surfaces of the UCD test specimen acted as targets. Aluminum foil was adhered to the uPVC discs using silicone grease. The transducer face was moved normal to the target and the actual displacement that had occurred was precisely measured using a laser system which had resolution and accuracy values of the order of  $10^{-9}$  and  $10^{-8}$  mm, respectively.

The proximity transducers were calibrated to a measurement accuracy of  $1.0 \times 10^{-5}$  mm, which corresponds to an accuracy in terms of the radial and circumferential normal strains of  $7 \times 10^{-5}$  % (computed for the UCD specimen dimensions using Eqs. 1 and 2). The tests and calibration procedures were carried out in a temperature-controlled environment at  $20 \pm 2^\circ\text{C}$ .

Typical calibration data for the outer proximity transducer (convex target) and the inner proximity transducer (concave target) are shown in Fig. 7.



(a) Outer proximity transducer and convex target.



(b) Inner proximity transducer and concave target.

Figure 7. Calibration curves.

Both transducer responses were non-linear and best fitted by fourth order polynomials ( $R^2 = 0.9999$ ) using the method of least squares (similar approach used by Hird and Yung (1989)). The calibration equations were coded and used in the UCD HCA control program (O'Kelly and Naughton, 2005a). The measurement accuracy was found to be 0.1% of the full-scale output.

The measurement accuracy can be further improved, if necessary, by calibrating the transducers over a smaller range or by reducing the transducer offset (Kaman Instrumentation Corporation, 1986), particularly in the case of the outer proximity transducer (convex target). Such improvements are desirable from a control standpoint for stress path measurements over the pseudo elastic range. For example, the torsional shear stress induced in the specimen under the action of an applied torque is particularly sensitive to the radial displacements of the inner and outer specimen wall surfaces.

The electrical stability of the transducer outputs with elapsed time was also assessed by recording the instrument readings at five-minute intervals over a 24-hour period. The standard deviation was less than 0.5% of the mean output voltage which was considered adequate.

A second series of tests were performed in which the proximity transducers were calibrated in air in order to assess the magnitude of the error that could arise. The data curves for calibration in air differed from that in water by about 0.09 mm over the measurement range of 0.5 to 5.0 mm (Fig. 8), equating to a measurement error of about 1.5% full scale, which is significant in the determination of the small strain stiffness of geomaterials.

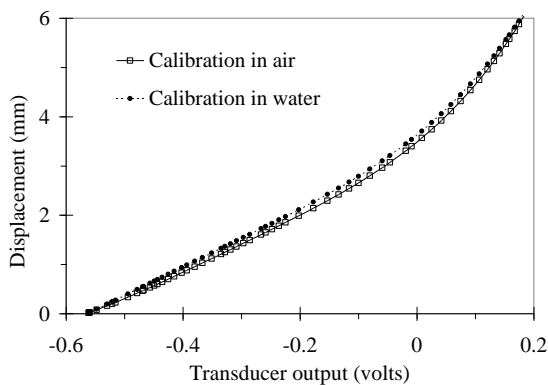


Figure 8. Comparison of calibration in water and in air.

Menkiti (1995) also found that different calibration curves were obtained for calibration of a proximity transducer (9.5 mm range) in air and in water. The magnitude of the error reported by Menkiti (1995) was greater than that for the UCD HCA set up (6.5 mm range) due to the larger measurement range.

## 6 PROVING TESTS

A fully saturated sand specimen (35.5 mm inner radius, 50.0 mm outer radius and 200 mm in length) was prepared in the UCD HCA using a wet pluviation technique (O'Kelly and Naughton, 2005c) and densified to an initial void ratio of 80.8% (medium to dense state). The properties of the uniform medium sand material (white Leighton Buzzard sand comprising sub-angular grains) have been reported elsewhere by O'Kelly and Naughton (2005b, c).

The test specimen was isotropically consolidated to a mean effective stress ( $p'$ ) of 200 kPa, against an applied backpressure of 150 kPa. The specimen was then anisotropically consolidated, namely:

1. The effective stress ratio ( $R'$ ) and the intermediate principal stress parameter ( $b$ ) were linearly

increased from  $R' = 1.0$  to 1.5, and  $b = 0.0$  to 0.5, with  $p'$  remaining fixed at 200 kPa.

2. Next, the orientation of the major principal stress ( $\alpha_\sigma$ ) was smoothly rotated from  $\alpha_\sigma = 0$  (vertical direction) to  $\alpha_\sigma = 45^\circ$ , with the values of  $p'$ ,  $R'$  and the  $b$  parameter remaining constant.
3. Finally, the  $R'$  value was increased from  $R' = 1.5$  to 2.5, with the values of  $p'$ , the  $b$  parameter and  $\alpha_\sigma$  remaining constant.

The stress path was followed by stepping between a series of intermediate target stress points located along the prescribed stress path (O'Kelly and Naughton, 2005a). The smooth control achieved for the torsional shear stress ( $\tau_{z\theta}$ ) and the effective normal stresses induced in the axial ( $\sigma'_z$ ), radial ( $\sigma'_r$ ) and circumferential ( $\sigma'_\theta$ ) directions are shown in Fig. 9 (actual values of the mean stress components were within 2.5% of the targeted values along the stress path).

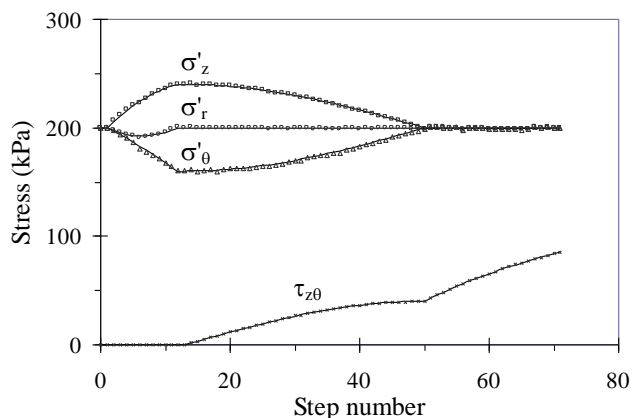
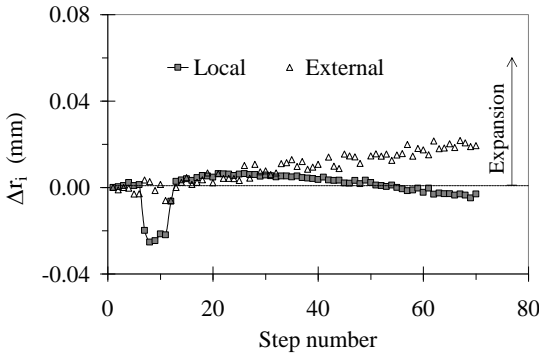


Figure 9. Smooth variation of stress components in targeting the stress path.

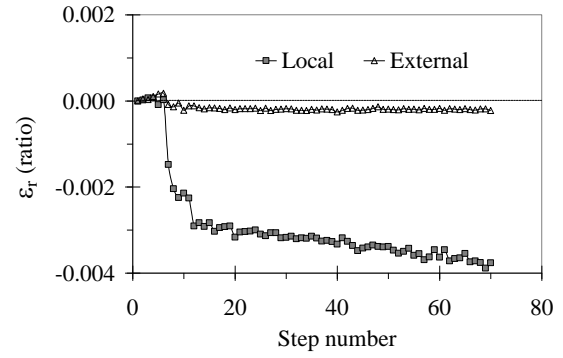
The control program calculated the states of stress and strain in the test specimen based on the deformation response measured by the local instrumentation (O'Kelly and Naughton, 2005a).

Figure 10 shows the radial displacements of the inner and outer specimen wall surfaces directly measured using the proximity transducers. Also included are the radial displacements computed from the overall axial deformation and volume changes of the specimen and its inner bore cavity which were measured by the external instrumentation.

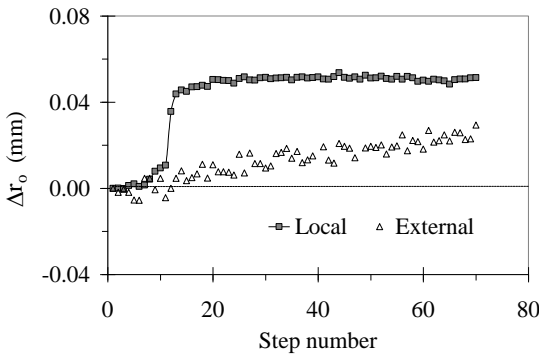
The rubber membranes that enclosed the inner and outer specimen wall surfaces were 0.38 mm in thickness. The volume change measurements were correct for the effects of membrane penetration using the method developed by Sivathayalan and Vaid (1998) and coded in the HCA control program (Naughton and O'Kelly (2003); O'Kelly and Naughton (2005a, c)).



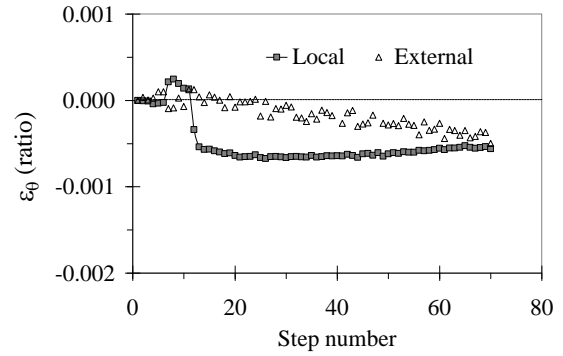
(a) Inner wall surface.



(a) Mean radial normal strain.



(b) Outer wall surface.



(b) Mean circumferential normal strain.

Figure 10. Radial displacements of specimen wall surfaces.

Figure 11. Strain responses.

The radial and circumferential normal strains shown in Fig. 11 are the mean values computed from the measured wall surface displacements using Eqs. 1 and 2.

O'Kelly and Naughton (2005b) have shown that the axial strains measured using the local (electrolevel inclinometers attached to outer specimen wall surface) and external instrumentation are in reasonable agreement. However, Fig. 11 indicates that significant differences can occur between the radial displacements of the specimen wall surfaces (and hence the radial and circumferential normal strains) determined on the basis of the local (i.e. proximity transducers) and external measurements.

The local measurements over the central, uniformly stressed gage length give the true strain response. Significant errors occurred in the external measurements, particularly for the outer wall displacement (Fig. 10b), due to inaccuracies in measuring the actual volume changes of the specimen and its inner bore cavity; specimen end restraint effects and the fact that the wall displacements are calculated as mean values over the full specimen volume.

The error is compounded in the case of the outer radial wall displacement (mean value computed on the basis of two volume change measurements rather than the one volume change measurement in the case of the inner radial wall displacement).

## 7 SUMMARY AND CONCLUSIONS

Non-contacting proximity transducers are ideally suited for local measurements of the deformation response of a free boundary surface. Proximity transducers have been used in this study to accurately measure the radial and circumferential normal strain responses of the test specimen in a hollow cylinder apparatus (HCA). The radial displacements of the inner and outer wall surfaces of the specimen are measured by the proximity transducers over its central, uniformly stressed zone.

The complete strain response (pseudo elastic range to failure condition) is fully captured using the proximity transducers, which have a measurement range of 6.0 mm and a resolution of  $1.1 \times 10^{-6}$  mm (more than an order of magnitude improvement in the resolution values reported for similar set ups in geotechnical literature). Precision gearing is used to relocate the instruments from outside the pressure cell during the course of a test.

The transducers were calibrated using an optical table and a laser distance-measurement system to achieve the necessary measurement accuracy of  $1.0 \times 10^{-5}$  mm (radial and circumferential normal strains of  $7 \times 10^{-5}$  %). The measurement accuracy can be further improved by calibrating the transducers over a smaller range, and in the case of the outer proximi-

ty transducer, by reducing the transducer offset distance. Such improvements are desirable from a control standpoint in conducting stress path measurements over the pseudo elastic range.

The proximity transducers were calibrated in water (in service condition) since the transducer response is influenced by the operating medium. For example, the calibration curves for calibration in water and in air differed by about 0.09 mm (about 1.5% full scale), which is a significant error in terms of small strain measurements. The calibration curves were non linear (best fitted by fourth order polynomials) and strongly influenced by the target curvature (convex and concave for the outer and inner specimen wall surfaces, respectively).

External measurements recorded during generalized stress path tests on saturated sand specimens in the HCA included significant errors, particularly in the case of the outer wall displacement, due to: (a) apparatus compliance; (b) specimen end restraint and bedding effects; (c) inaccuracies in measuring the volume change of the specimen and its inner bore cavity; and (d) the fact that the specimen wall displacements are calculated as mean values over the full specimen volume.

The proximity transducer set ups and calibration procedure described in this study can be equally applied to provide a cost-effective, reliable and accurate distance measurement system in other geotechnical laboratory applications.

## ACKNOWLEDGMENTS

The authors would like to thank Dr. Tom Widdis and Professor Eugene O'Brien (University College Dublin) for their support during the course of this research. The lead author is also grateful for funding received under the Pierse-Newman Scholarship in Civil Engineering from University College Dublin.

## REFERENCES

- Baldi, G., Hight, D. W. and Thomas, G. E. (1988). "A reevaluation of conventional triaxial test methods", *Advanced Triaxial Testing of Soils and Rock*, ASTM STP977, Philadelphia.
- Brown, S. F., Austin, G. and Overy, R. F. (1980). "An instrumented triaxial cell for cyclic loading of clays", *ASTM Geotechnical Testing Journal*, Vol. 3, No. 4, pp. 145–152.
- Clayton, C. R. I. and Khatrush, S. A. (1986). "A new device for measuring local axial strains on triaxial specimens", *Géotechnique*, Vol. 36, No. 4, pp. 593–597.
- Cuccovillo, T. and Coop, M. R. (1997). "The measurement of local axial strains in triaxial tests using LVDTs", *Géotechnique*, Vol. 47, No. 1, pp. 167–171.
- Hight, D. W., Gens, A. and Symes, M. J. (1983). "The development of a new hollow cylinder apparatus for investigating the effects of principal stress rotation in soils", *Géotechnique*, Vol. 33, No. 4, pp. 355–383.
- Hird, C. C. and Yung, P. C. Y. (1989). "The use of proximity transducers for local measurements in triaxial tests", *ASTM Geotechnical Testing Journal*, Vol. 12, No. 4, pp. 292–296.
- Jardine, R. J., Symes, M. J. and Burland, J. B. (1984). "The measurement of soil stiffness in the triaxial apparatus", *Géotechnique*, Vol. 34, No. 3, pp. 323–340.
- Kaman Instrumentation Corporation (1986). "Application of a precision measurement technology", *Kaman Measuring Systems Seminar Workbook*, SWB 865.
- Lo Presti, D. C. F., Pallara, O., Lancellotta, R., Armandi, M. and Maniscalco, R. (1993). "Monotonic and cyclic loading behavior of two sand at small strains", *ASTM Geotechnical Testing Journal*, Vol. 16, No. 4, pp. 409–424.
- Menkiti, O. C. (1995). "Behaviour of clay and clayey-sand with particular reference to principal stresses rotation", PhD thesis, University of London (Imperial College).
- Naughton P. J. and O'Kelly B. C. (2007). "Stress non-uniformity in a hollow cylinder torsional sand specimen", *Geomechanics and Geoengineering*, Vol. 2, No. 2, pp. 117–122.
- Naughton P. J. and O'Kelly B. C. (2003). "The anisotropy of Leighton Buzzard sand under general stress conditions", *Proceedings Third International Symposium on Deformation Characteristics of Geomaterials*, Lyon, 1, pp. 285–292.
- O'Kelly B. C. and Naughton P. J. (2003). "Development of a new hollow cylinder apparatus for generalised stress path testing", *Ground Engineering*, Vol. 36, No. 7, pp. 26–28.
- O'Kelly B. C. and Naughton P. J. (2005a). "Closed-loop control of a hollow cylinder apparatus", *Proceedings Symposium on Innovative Experimental Techniques at the ASCE/ASME/SES Conference on Mechanics and Materials*, Baton Rouge, Louisiana, USA.
- O'Kelly B. C. and Naughton P. J. (2005b). "Development of a new hollow cylinder apparatus for stress path measurements over a wide strain range", *ASTM Geotechnical Testing Journal*, Vol. 28, No. 4, pp. 345–354.
- O'Kelly B. C. and Naughton P. J. (2005c). "Engineering properties of wet-pluviated hollow cylindrical specimens", *ASTM Geotechnical Testing Journal*, Vol. 28, No. 6, pp. 570–576.
- O'Kelly B. C. and Naughton P. J. (2008). "Measuring shear strain in a hollow cylinder apparatus using electrolevel-inclinometer gages", *Proceedings Fourth International Symposium on Deformation Characteristics of Geomaterials*, Atlanta, USA.
- Rechenmacher, A. L. and Finno, R. J. (2004). "Digital image correlation to evaluate shear banding in dilative sands", *ASTM Geotechnical Testing Journal*, Vol. 27, No. 1, pp. 13–22.
- Scholey, G. K., Frost, J. D., Lo Presti, D. C. F. and Jamiolkowski, M. (1995). "A review of instrumentation for measuring small strains during triaxial testing of soil specimens", *ASTM Geotechnical Testing Journal*, Vol. 18, No. 2.
- Sivathayalan, S. and Vaid, Y. P. (1998). "Truly undrained response of granular soils with no membrane penetration effects", *Canadian Geotechnical Journal*, Vol. 35, pp. 730–739.
- Symes, M. J. and Burland, J. B. (1984). "Determination of local displacements on soil samples", *ASTM Geotechnical Testing Journal*, Vol. 7, No. 2, pp. 49–59.
- Tatsuoka, F., Muramatsu, M. and Sasaki, T. (1983). Closure to "Cyclic undrained stress-strain behaviour of dense sands by torsional simple shear tests", *Soils and Foundations*, Vol. 23, No. 3, pp. 142–145.